

Measurement Device for Inverter Output Impedance Considering the Coupling Over Frequency

Tommi Reinikka
Tampere University
Faculty of Information Technology
and Communication Sciences
Tampere, Finland
tommi.reinikka@tuni.fi

Tomi Roinila
Tampere University
Faculty of Information Technology
and Communication Sciences
Tampere, Finland
tomi.roinila@tuni.fi

Jian Sun
Center for Future Energy Systems
Rensselaer Polytechnic Institute
Troy, NY, USA
jsun@ecse.rpi.edu

Abstract—Inverter output impedance is an important parameter for assessing the stability of a grid-connected system. However, measuring the inverter output impedance is not straightforward because the impedance is affected by a nonlinear coupling over frequency. In a typical measurement setup the inverter output impedance is measured by applying an external perturbation injected by an additional (source) inverter. Under non-ideal conditions, the inverter under test produces undesired (mirrored) frequency harmonics which interact with the source inverter thus affecting the measured output impedance. This paper proposes a measurement technique that decouples the mirrored frequency harmonics during the impedance measurement. In the method, the impedance of the source inverter performing the measurement is shaped so that the coupling over frequency is minimized. By applying this method, the inverter output impedance can be accurately and reliably measured in non-ideal conditions.

Index Terms—Mirrored Harmonic, Impedance Measurement, Inverter, Output Admittance, Coupling over Frequency

I. INTRODUCTION

Stability analysis of grid-connected systems has become an important topic due to the continuous increase in the use of renewable energy sources, which are often connected to the power grid through inverters. Due to the increased number of inverter-connected resources the dynamics of the power grid has started to change. One of the main issues studied has been the harmonic resonance between the inverter and the grid. The harmonic resonance is an indication of lack of system stability margin and may lead to instability [1].

The harmonic resonance and system stability can be studied by applying impedance-based stability criterion [2]. The criterion has become popular as it only requires the information of the inverter output impedance and the grid impedance. In the method, the ratio of the impedances is calculated after which the Nyquist stability criterion is applied to determine the stability. The stability criterion requires that the grid impedance and the inverter output impedance are accurately measured over a wide frequency band.

Measuring the inverter output impedance can be performed by applying an additional inverter acting as a perturbation source. The perturbation is placed on top of the source inverter fundamental voltage(s) or current(s). The resulting current and voltage responses are measured from the inverter under test

and Fourier techniques are applied to extract the corresponding frequency components. The impedance is then determined by the ratio between the measured voltage(s) and current(s). The measurement is straightforward with low-power inverters as the measurement device can often be assumed to be close to an ideal source [3]. The impedance measurement is, however, not feasible with high-power systems as the source impedance of the measurement device can affect the measurement [4]. The main challenge is that the inverter under test produces additional mirrored harmonic response through transfer admittance. The mirrored harmonic response interacts with the source impedance and changes the output impedance of the inverter under test [5].

In order to obtain accurate information of the inverter output impedance the coupling over frequency caused by the mirrored response must be compensated. The effect of the coupling over frequency can be avoided by ensuring a low source impedance compared to the output impedance of the inverter under test. This can be achieved by using a device rated a magnitude higher than the inverter under testing. However, when reaching multimewatt power levels, increasing the source inverter rating becomes unreasonable.

This paper proposes an algorithm which applies active power filtering methods to detect and cancel out the mirrored harmonic voltage response from the measurements. The algorithm effectively shapes the source impedance of the measurement device to a lower level at the mirrored harmonic frequency, and as such, decouples the mirrored harmonic from affecting the inverter output impedance measurement. The same idea was earlier applied by using an additional shunt or series active power filter [6]. However, the practical requirements are difficult to fulfill for implementing an accurate control with a narrow bandwidth near the fundamental frequency by using an active power filter design.

The remainder of the work is organized as follows. Section II explains how the mirrored harmonic response is generated. Section III shows the design of the measured device with the mirrored harmonic cancellation. Section IV presents the analytical model for the measurement device. Section V presents simulated impedance measurement in which the mirrored harmonic response is decoupled. Finally, section VI

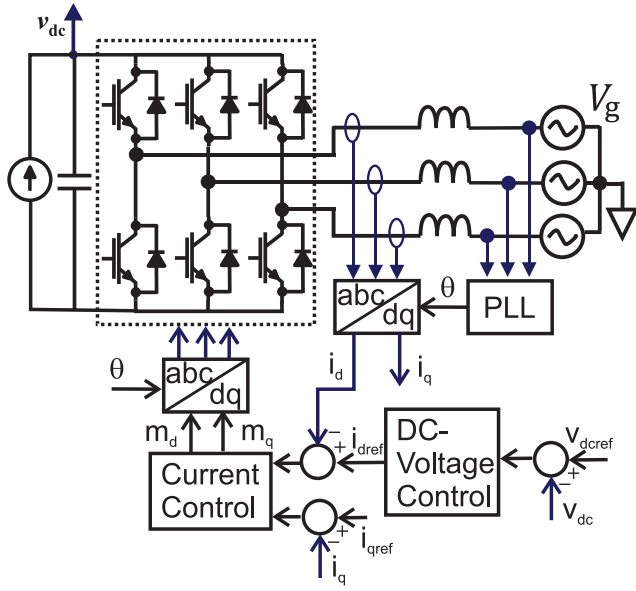


Fig. 1. The layout of the inverter under test

draws the conclusion.

II. COUPLING THROUGH MIRRORED HARMONIC RESPONSE

The inverter under test is a three-phase 2-level voltage source converter. Fig 1 shows the layout and the control design of the inverter under test. The AC-side is modeled as an L-filter and the DC-side is modeled as an DC-bus capacitor connected to an ideal current source. The coupling over frequency in the inverter can be modeled by a multi-harmonic linearization [5]. The multiharmonic analysis shows that with a 2-level voltage source converter, the DC-bus and PLL dynamics of the inverter have a non-linear response at the frequency of $2f_1 - f_p$, where f_1 is the fundamental frequency and f_p is the perturbation frequency [9]. The non-linear response interacts with the source impedance causing an additional feedback to the original perturbation frequency.

Perturbing the output voltage of the 2-level VSC under test with a positive-sequence voltage perturbation v_p causes a current response through the inverter output admittance $Y(s)$. The output admittance can be split into different components. Fig. 2 shows the block diagram how the VSC current response is affected. The admittance components can be found more in detail in [9]. The positive-sequence AC-voltage perturbation at frequency f_p has a response Y_{a1} to the output current at the perturbation frequency f_p and a response Y_{a2} at the mirrored frequency $2f_1 - f_p$. In addition there is a DC-current response at frequency $f_p - 2f_1$. The DC-bus is not ideal and has an impedance Z_{00} which causes the DC-voltage to be perturbed at $f_p - 2f_1$. The response to the DC-bus voltage perturbation can be split similarly to the AC-perturbation. The DC-voltage has a response Y_{01} to the AC-current at the frequency f_p , a response Y_{02} at the mirrored frequency $2f_1 - f_p$ and a response Y_{00} to the DC-current at the frequency $f_p - 2f_1$. Combining

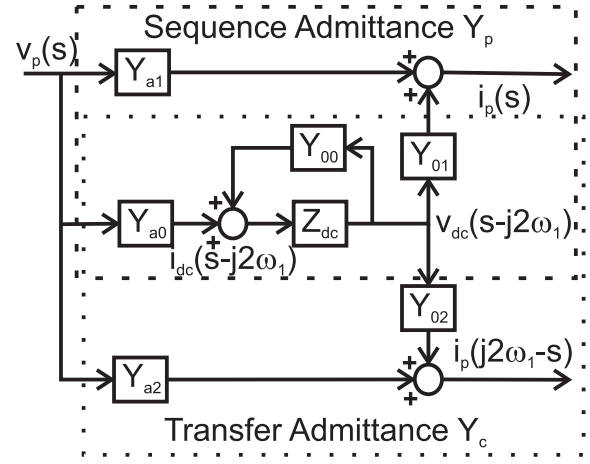


Fig. 2. Block diagram of inverter output admittance Y_p and transfer admittance Y_c

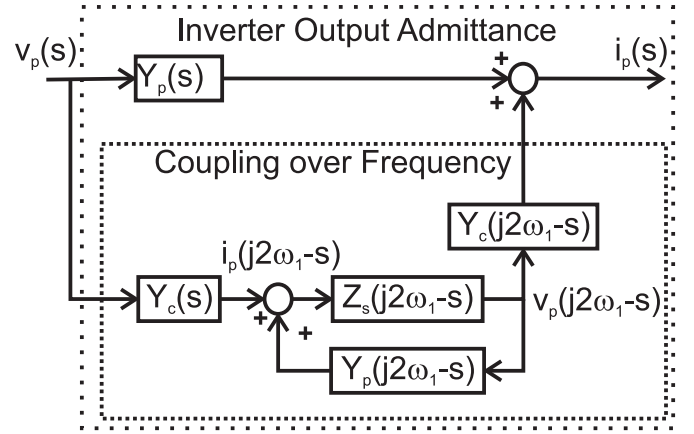


Fig. 3. The current response $i_p(s)$ is affected by the nonlinear current response $i_p(s)$ through the source impedance

the responses together forms the output admittance Y_p to the perturbation frequency and the transfer admittance Y_c to the mirrored frequency as

$$Y_p = -Y_{a1}(s) + \frac{Y_{a0}Y_{01}(s - j\omega_1)}{Y_{00}(s - j\omega_1) + Y_{dc}(s - j\omega_1)} \quad (1)$$

$$Y_c = -Y_{a2}(s) + \frac{Y_{a0}Y_{02}(s - j\omega_1)}{Y_{00}(s - j\omega_1) + Y_{dc}(s - j\omega_1)} \quad (2)$$

The coupling over frequency can be calculated using the output admittance Y_p , transfer admittance Y_c and the source admittance Z_s . Fig. 3 shows the current response $i_p(s)$ with the effect of the nonlinear current response included. The transfer admittance Y_c results in a current response as

$$\hat{i}_p(s - j\omega_1) = Y_c(s)\hat{v}_p(s) \quad (3)$$

The non-ideal source admittance Y_s causes the following mirrored harmonic voltage response which interacts with the inverter under test.

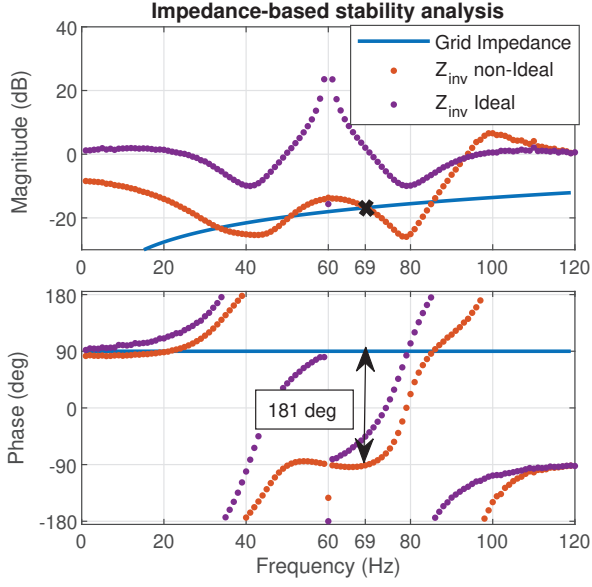


Fig. 4. Inverter output impedance without the grid affected dynamics (violet dots), with grid affected dynamics (orange dots) and the power grid impedance with SCR 1.26 (blue line)

$$\hat{v}_p(s - j\omega_1) = \frac{Y_c}{Y_g(s - j\omega_1) + Y_p(s - j\omega_1)} \hat{v}_p \quad (4)$$

The mirrored harmonic voltage response further causes a current response from the inverter under test through the transfer admittance at the mirrored harmonic frequency as

$$\hat{i}_r(s) = Y_c(s - j\omega_1) * \hat{v}_p \quad (5)$$

The additional current component at the perturbation frequency changes the output admittance of the inverter. The admittance component Y_{p2} caused by the coupling over frequency can be presented as

$$Y_{p2} = -\frac{Y_c(s)Y_c^*(s - j\omega_1)}{Y_c^*(j2\omega_1 - s)Y_p^*(s - j\omega_1)} \quad (6)$$

The inverter output admittance considering the coupling over frequency can be calculated by combining (1) and (6).

$$Y(s) = Y_p(s) - \frac{Y_c(s)Y_c^*(s - j2\omega_1)}{Y_g(s - j2\omega_1) + Y_p^*(s - j2\omega_1)} \quad (7)$$

where ω_1 is the grid angular velocity and * denotes complex conjugate. To calculate the effect of the source impedance the VSC output admittance $Y_p(s)$ and $Y_c(s)$ must be known in ideal conditions. To measure the positive sequence component Y_p and the transfer admittance $Y_c(s)$ as with an ideal source, the latter part of the equation must be small compared to Y_p . This can be achieved by increasing the source admittance $Y_s(j2\omega_1 - s)$.

The effect of the coupling over frequency is illustrated in Figs. 4 and 5. The inverter is connected to a power grid (SCR =

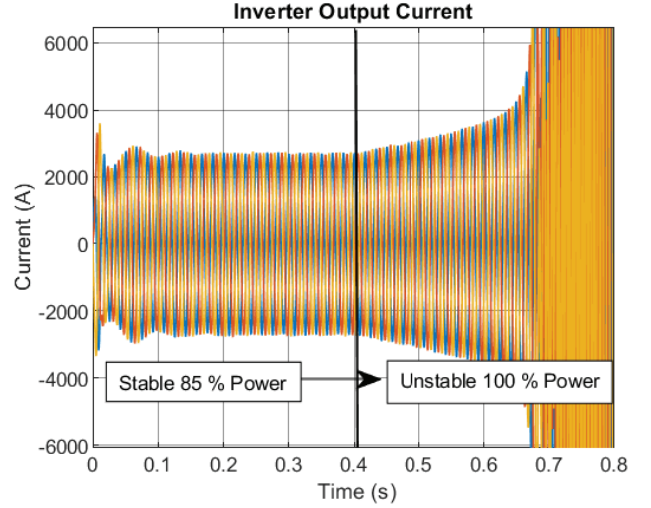


Fig. 5. The inverter output current goes unstable when the output power is increased to 100 % at 0.4 s.

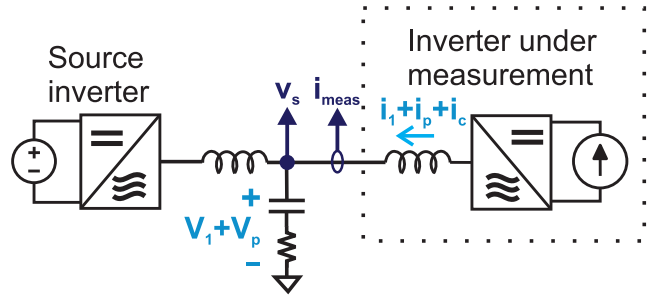


Fig. 6. The impedance measurement setup

1.26) and fed by an ideal source. The SCR is set to a very low value to efficiently demonstrate the affected impedance. If the output impedance is measured by using an ideal source, and then used for the impedance-based stability assessment, the system shows stable operation. However, when the coupling over frequency is included as in (7), the system is predicted to be unstable. Fig. 5 shows the inverter becoming unstable when the output power is increased from 85 to 100 at 0.4 s. The impedance-based stability analysis cannot be used unless the effect of the coupling over frequency is considered. In order to calculate the effect of the source admittance Y_s with (7), the inverter output impedance Y_p and transfer admittance Y_c must be known as in an ideal grid connection.

III. CONTROL DESIGN

In the proposed measurement setup the inverter under test is fed by an external source inverter. The source inverter controls the fundamental voltage, performs the voltage perturbation and cancels out the mirrored harmonic voltage response. Fig. 6 shows the layout of the measurement setup. The measurement device is designed as a three-phase inverter with an LC-filter. The LC-filter capacitor branch voltage is used as a direct control over the output voltage of the inverter. The mirrored

harmonic component is extracted from the same point as the controlled output voltage. It is assumed that there is no isolation transformer required in the setup and the impedance between the measurement device and the inverter under measurement is negligible. If there was a significant impedance between the devices, the mirrored harmonic compensation should be performed at the input terminal of the inverter under measurement.

The perturbation is carried out by injecting a sequence-domain voltage to the output reference of the inverter controller. The perturbation signal can be transformed from sequence-domain to abc-domain signals with a transform matrix

$$T_{pn0\text{-to-abc}} = \begin{bmatrix} 1 & a & a^2 \\ 1 & a^2 & a \\ 1 & 1 & 1 \end{bmatrix} \begin{bmatrix} v_p \\ v_n \\ v_0 \end{bmatrix} \quad (8)$$

where $a = e^{i2/3\pi}$. The VSC sequence-domain output admittance and the transfer admittance can be calculated from the output voltage and output current measurement as

$$\begin{bmatrix} Y_p \\ Y_c \end{bmatrix} = \begin{bmatrix} I(s)/V(s) \\ I(2f_1 - s)/V(s) \end{bmatrix} \quad (9)$$

The measurement device is a 3-phase inverter with similar rating as the inverter under test. The rating is chosen to be around the same magnitude to efficiently show the issues caused by the coupling over frequency. The measurement device is built with an LC-filter and the controlled output voltage is the voltage over the capacitor branch. The power stage can be modeled with the over the LC-filter by using (10)-(12). The inputs of the system are the output current i_o and the modulation index m . Inductor current i_l and capacitor voltage v_c are the states and the output voltage v_o is the output of the system.

$$L \frac{d}{dt} \begin{bmatrix} i_{la} \\ i_{lb} \\ i_{lc} \end{bmatrix} = v_{DC} \begin{bmatrix} m_a \\ m_b \\ m_c \end{bmatrix} - v_n - \begin{bmatrix} v_{oa} \\ v_{ob} \\ v_{oc} \end{bmatrix} \quad (10)$$

$$C \frac{d}{dt} \begin{bmatrix} v_{va} \\ v_{vb} \\ v_{vc} \end{bmatrix} = \begin{bmatrix} i_{oa} \\ i_{ob} \\ i_{oc} \end{bmatrix} - \begin{bmatrix} i_{la} \\ i_{lb} \\ i_{lc} \end{bmatrix} \quad (11)$$

$$\begin{bmatrix} v_{oa} \\ v_{ob} \\ v_{oc} \end{bmatrix} = \begin{bmatrix} v_{ca} \\ v_{cb} \\ v_{cc} \end{bmatrix} + \begin{bmatrix} i_{ca} \\ i_{cb} \\ i_{cc} \end{bmatrix} R_d \quad (12)$$

The system is considered balanced and, as such, the equations are reduced to single-phase equivalent. In the frequency domain the transfer functions are as follows

$$V_{ca}(s) = \frac{1}{sC} I_{oa} - \frac{1}{sC} I_{la} \quad (13)$$

$$I_{la}(s) = \frac{1}{sL} V_{oa}(s) - \frac{1}{sL} K_m V_{dc} M_a(s) \quad (14)$$

$$V_{oa}(s) = V_{ca}(s) + I_{oa}(s) R_d - I_{la}(s) R_d \quad (15)$$

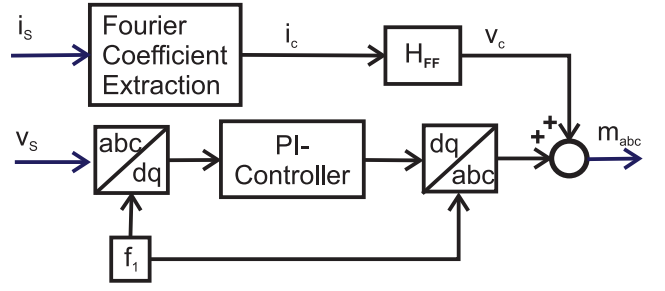


Fig. 7. Controller layout for the mirrored harmonic compensation with a current feedforward

Combining (13), (14), (15) yields the following transfer functions

$$Z_{io-o} = \frac{\hat{v}_{oa}}{\hat{i}_{oa}} = \frac{\frac{1}{sC} + R_d}{s^2 LC + \frac{R_d}{sL} + 1} \quad (16)$$

$$H_{co-o} = \frac{\hat{v}_{oa}}{\hat{m}_a} = \frac{(\frac{1}{s^2 LC} + \frac{R_d}{sL}) K_m V_{dc}}{\frac{1}{s^2 LC} + \frac{R_d}{sL} + 1} \hat{m}_a \quad (17)$$

$$\hat{v}_{oa} = Z_{io-o} \hat{i}_{oa} + H_{co-o} \hat{m}_a \quad (18)$$

where H_{co} is the open-loop output current to output voltage transfer function and H_{co} is the open-loop modulation index to output-voltage transfer function. The control to output transfer function H_{co} can be used to tune the voltage controller H_v .

The inverter output voltage is controlled by a dq-domain PI-controller. The mirrored harmonic mitigation can be performed in several ways. Algorithms based on current feedforward and voltage feedback control are proposed in this paper. As there is no PLL required and the DC-bus is considered to be controlled with another much faster or ideal device, there is no coupling over frequency present in the measurement device and only the linear response must be considered for the mirrored harmonic voltage compensation.

A. Current Feedforward

The simplest method to reduce the voltage response of the measurement device is to use a current feedforward as a virtual impedance to mitigate the voltage response at the output terminal of the device. The method requires extracting the mirrored harmonic current component and the information on the response of the measurement device at the mirrored harmonic frequency. The analytical response is simplified as the measurement is performed at steady-state and there are no external components changing the operation state and the current component extraction does not need to be performed continuously.

The required voltage injection is calculated from (18) and assuming the steady-state voltage error to be zero. The feedforward gain is calculated so that the effect of the sensed mirrored harmonic current component to the output voltage at the output terminal of the measurement device is equal to

the effect of mirrored harmonic current. The resulting voltage response equals to zero as

$$Z_{i_o-o}(j\omega_c)I_{oa}(j\omega_c) + H_{co-o}(j\omega_c)M_a(j\omega_c) = 0 \quad (19)$$

As the steady-state error is assumed to be zero the voltage controller feedback does not affect the calculation of the error and the feedforward gain H_{FF} is designed to mitigate the effect of the mirrored harmonic current. The steady-state value of the modulation index M_a is composed only of the feedforward and can be presented as

$$M_a(j\omega_c) = K_m V_{dc} F F_{gain} I_{oa}(j\omega_c) \quad (20)$$

Combining (19) and (20) allows calculating the required feedforward gain as

$$H_{FF} = -\frac{\frac{1}{sL} + R_d}{\left(\frac{1}{s^2 LC} + \frac{R_d}{sL}\right)K_m V_{dc}} \quad (21)$$

Applying (21) requires information on the mirrored harmonic frequency component from the output current. The method is a steady-state correction, which means the mirrored-harmonic current component can be extracted from prior measurements. The Fourier coefficients can be extracted from the current measurements using the following equations

$$a_n = \frac{2T_s}{P} \sum_{n=1}^N s(x) * \cos(2\pi x \frac{n}{P}) \quad (22)$$

$$b_n = \frac{2T_s}{P} \sum_{n=1}^N s(x) * \sin(2\pi x \frac{n}{P}) \quad (23)$$

where n is the Fourier coefficient number, N is the length of the data points, P is the time of the measurements, x is the time of the data point and $s(x)$ is the value of the data point. The amplitude of the mirrored harmonic component can be extracted from the Fourier coefficients of the mirrored harmonic frequency. The phase can be determined by comparing the phase between the fundamental component and the mirrored harmonic component. Multiplying the extracted frequency component with the feedforward gain gives the required feedforward voltage injection for the mitigation of the mirrored harmonic voltage response.

B. Voltage Feedback

Another method to control the mirrored harmonic voltage to zero is a parallel voltage-feedback controller. The mirrored harmonic voltage component is extracted using a narrow low-pass filter and then controlled to zero. The modulation index M_a can be presented with the transfer functions of the voltage controller and the mirrored harmonic cancellation resulting in the transfer function of the controller as

$$M_a(s) = -(H_v(s - \omega_1) + H_{mh}(s - \omega_{mh}))V_{oa}(s) \quad (24)$$

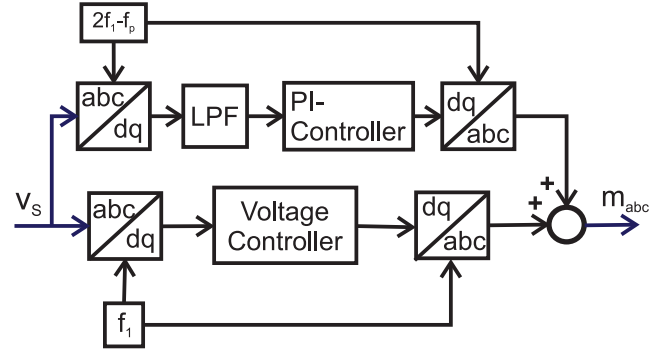


Fig. 8. Controller layout for the mirrored harmonic compensation with the voltage feedback control

TABLE I
MEASUREMENT DEVICE PARAMETERS

Parameter	Symbol	Value
APF Apparent Power	S_s	3 MVA
APF Switching Frequency	f_{sw}	10 kHz
Inverter DC-voltage	V_{DC}	1500 V
LC-filter inductor	L_f	88 μH
LC-filter capacitor	C_f	6.68 mF
LC-filter damping resistor	R_d	0.16 Ω
Controller Kp	K_{pf}	0.32
Controller Ki	K_{if}	141

The mirrored harmonic extraction is performed by dq-transforming the voltage measurement at the mirrored harmonic frequency and filtering the signal by using a 5th-order Butterworth low-pass filter. The filtered signal is used as the controller feedback for the PI-controller. The mirrored harmonic controller can be added to the fundamental voltage controller transfer function as they are connected in parallel. The mirrored harmonic controller branch can be modelled as

$$H_{mh}(s - \omega_{mh}) = LPF(s - \omega_{mh}) \left(Kp + \frac{Ki}{(s - \omega_{mh})} \right) V_{oa} \quad (25)$$

As there is no PLL and the DC-bus voltage is assumed to be controlled through a significantly faster DC-converter the coupling over frequency is considered insignificant to the measurement device. If, however, the DC-bus voltage control has slow dynamics the coupling over frequency cannot be ignored for the measurement device.

IV. SOURCE IMPEDANCE CHARACTERIZATION

The operation of the impedance measurement device is tested in a simulation environment. The device is a 3-phase 2-level inverter with a 3 MW rating, which is analyzed by connecting it to an ideal current source and measuring the output impedance of the device. First, the measurement is performed so that the compensation is at the measured frequency. Then, the compensation is set around the compensation frequency. The parameters of the measurement device are shown in Table I. The parameters for the feedforward compensation are shown in Table II and for the feedback compensation in Table III.

TABLE II
FEEDFORWARD COMPENSATION PARAMETERS

Parameter	Symbol	Value
Measurement time	t_{ff}	1 s
Feedforward Sampling Frequency	f_{sff}	10000 Hz

TABLE III
FEEDBACK COMPENSATION PARAMETERS

Parameter	Symbol	Value
Lowpass filter Bandwidth	f_{bw}	5 Hz
Controller Kp	K_{pc}	0.0893
Controller Ki	K_{ic}	1.12

Fig. 9 shows how different compensation methods reduce the output impedance of the measurement device. The impedance is measured from 1 Hz to 120 Hz, which is the range where the transfer admittance has been shown to have a major effect to the output impedance. The compensation frequency is set to the measured frequency at each point. The attenuation of the feedforward is approximately -20 to -30 db around the frequency of interest. The feedforward performance is dependent on the presence of modeling error, such as, delays caused by the PWM and control and the difference in the rated and real value of the filter components. The feedback compensation is much more effective, giving attenuation of over -80 db. However, when measuring near the fundamental voltage the attenuation is dependent on the performance of the narrowband-filter. As the fundamental voltage can be two magnitudes higher the narrowband filter must have a significant attenuation near to the cutoff-frequency to block the fundamental voltage passing through the compensation.

Fig. 10 shows the effect of the mirrored harmonic feedback compensation to the measurement device output impedance around the compensated frequency. The impedance is reduced

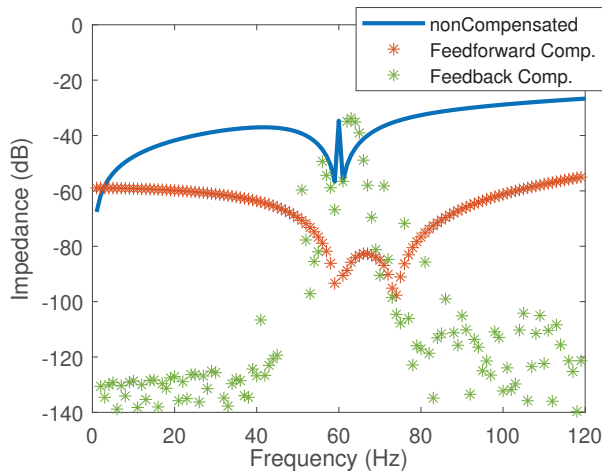


Fig. 9. The output impedance of the measurement device with feedforward compensation (orange stars), with feedback compensation (green stars) and without compensation (blue line)

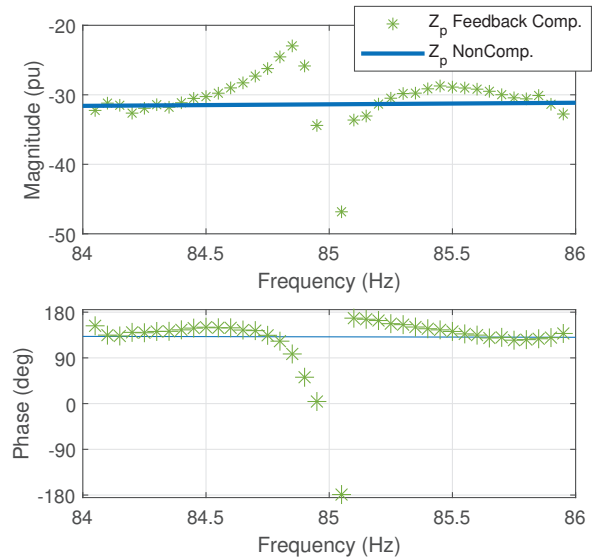


Fig. 10. The measurement device output impedance with the effect of feedback compensation at 85 Hz

TABLE IV
PARAMETERS OF THE INVERTER UNDER TEST

Parameter	Symbol	Value
APF Apparent Power	S_{apf}	3 MVA
APF Switching Frequency	f_{sw}	10 kHz
Inverter DC-voltage	V_{dc}	1500 V
L-filter inductor	L_f	1.3 mH
Current Controller Bandwidth	f_{cc}	300 Hz
DC-voltage Controller Bandwidth	f_{vc}	20 Hz
PLL Bandwidth	f_{PLL}	30 Hz

towards zero and the compensation has a phase difference of zero. However, around the compensated frequency the filtering of the mirrored harmonic component causes significant changes to the impedance magnitude and phase, and therefore, the stability of the measurement setup must be carefully considered.

V. MEASURING INVERTER OUTPUT IMPEDANCE

The measurement device is connected in series with another inverter. The inverter under test is designed to have similar rating and parameters as the measurement device. The inverter under test is a 3 MW inverter, and the measurement device is a voltage-controlled inverter with a similar power rating. The parameters of the inverter under test is shown in Table IV

Fig. 11 shows the inverter positive-sequence output-impedance measurement. The impedance measured with the source inverter is compared to the impedance measured with an ideal source. The comparison is made to both feedback and feedforward mirrored-harmonic-compensation methods. With the mirrored-harmonic voltage cancellation enabled for both methods the measured positive-sequence impedance accurately follows the impedance obtained by an ideal source over a wide frequency band. The feedback compensation has reduced performance near to the fundamental frequency. The error

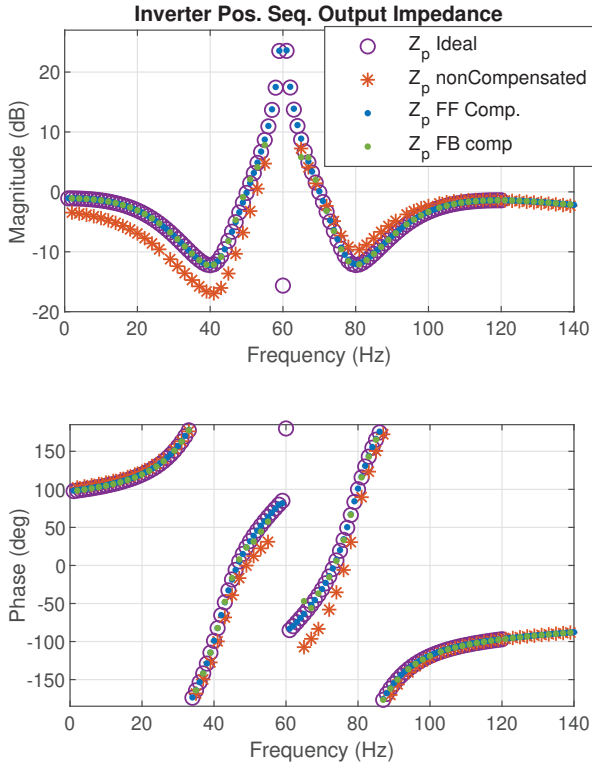


Fig. 11. Measured positive sequence inverter output impedance with an ideal source (purple circles), with no compensation (orange stars) and with both feedforward (blue dots) and feedback (green dots) compensation

increases as the used Butterworth lowpass-filter has bandwidth of 5 Hz. Narrower lowpass-filter allows the impedance to be measured closer to the fundamental frequency. However, that increases the measurement time and reduces the system robustness. Transfer admittance Y_c is not affected by the source impedance and it is not shown here due to lack of space. The feedforward compensation is accurate near the fundamental frequency as well. However, in real-world environment the model uncertainty increases, which may affect the performance of the method.

VI. CONCLUSION

The output impedance of a grid-connected inverter plays important role in the stability analysis of grid-connected systems. Measuring the inverter output impedance is, however, not straightforward because the impedance is affected by a nonlinear coupling over frequency when an additional source inverter is applied as an perturbation source in the measurement. This paper has proposed two methods to mitigate the effect of the nonlinear coupling; the current feedforward method and the voltage feedback method. In both methods, the impedance of the source inverter is shaped so that the nonlinear coupling is minimized in the impedance measurement of the inverter under test. The method based on the current feedforward is robust but the method requires an accurate model. On the

other hand, the method based on the voltage feedback is not dependent on the model accuracy but requires more careful consideration of the measurement setup stability. The future research includes hardware implementation of the proposed compensation methods.

REFERENCES

- [1] C. Li, "Unstable Operation of Photovoltaic Inverter From Field Experiences", IEEE Transactions on Power Delivery, vol. 33, no. 2, pp. 1013-1015, 2018.
- [2] J. Sun, "Impedance-Based Stability Criterion for Grid-Connected Inverters," IEEE Transactions on Power Electronics, vol. 26, no. 11, pp. 3075-3078, 2011
- [3] J. Jokipii, T. Messo and T. Suntio, "Simple method for measuring output impedance of a three-phase inverter in dq-domain," 2014 International Power Electronics Conference (IPEC-Hiroshima 2014 - ECCE ASIA), Hiroshima, pp. 1466-1470, 2014
- [4] I. Vieto and J. Sun, "Sequence Impedance Modeling and Converter-Grid Resonance Analysis Considering DC Bus Dynamics and Mirrored Harmonics," 2018 IEEE 19th Workshop on Control and Modeling for Power Electronics (COMPEL), pp. 1-8, Padua, 2018
- [5] J. Sun and H. Liu, "Sequence Impedance Modeling of Modular Multi-level Converters," in IEEE Journal of Emerging and Selected Topics in Power Electronics, vol. 5, no. 4, pp. 1427-1443, 2017
- [6] T. Reinikka, T. Roinila and J. Sun, "Accurate Measurement of Converter Sequence Impedance by Active Cancellation of Coupling over Frequency," 2019 4th IEEE Workshop on the Electronic Grid (eGRID), Xiamen, China, 2019, pp. 1-6
- [7] T. Messo, R. Luhtala, A. Aapro and T. Roinila, "Accurate Impedance Model of Grid-Connected Inverter for Small-Signal Stability Assessment in High-Impedance Grids," 2018 International Power Electronics Conference (IPEC-Niigata 2018 - ECCE Asia), Niigata, 2018, pp. 3156-3163
- [8] X. Guo, Z. Lu, B. Wang, X. Sun, L. Wang and J. M. Guerrero, "Dynamic Phasors-Based Modeling and Stability Analysis of Droop-Controlled Inverters for Microgrid Applications," in IEEE Transactions on Smart Grid, vol. 5, no. 6, pp. 2980-2987
- [9] I. Vieto, X. Du, H. Nian and J. Sun, "Frequency-domain coupling in two-level VSC small-signal dynamics," 2017 IEEE 18th Workshop on Control and Modeling for Power Electronics (COMPEL) pp. 1-8, Stanford, CA, 2017
- [10] H. Wang, I. Vieto and J. Sun, "A Method to Aggregate Turbine and Network Impedances for Wind Farm System Resonance Analysis," 2018 IEEE 19th Workshop on Control and Modeling for Power Electronics (COMPEL), Padua, 2018, pp. 1-8